Original Article
Mol Imaging Radionucl Ther 2023;32:94-102 DOI:10.4274/mirt.galenos.2022.97658

Value of Dynamic ^{18}F-FDG PET/CT in Predicting the Success of Neoadjuvant Chemotherapy in Patients with Locally Advanced Breast Cancer: A Prospective Study

Lokal İleri Evre Meme Kanserli Hastalarda Neoadjuvan Kemoterapi Yanıtı Öngörüsünde Dinamik ^{18}F-FDG PET/BT'nin Değeri: Prospektif Çalışma

Osman Kupik[1], Murat Tuncel[2], Pınar Özgen Kıratlı[2], Meltem Gülsün Akpınar[3], Kadri Altundağ[4], Figen Başaran Demirkazık[3], Belkıs Erbaş[2]

[1]*Muğla Training and Research Hospital, Clinic of Nuclear Medicine, Muğla, Turkey*
[2]*Hacettepe University Faculty of Medicine, Department of Nuclear Medicine, Ankara Turkey*
[3]*Hacettepe University Faculty of Medicine, Department of Radiology, Ankara, Turkey*
[4]*MKA Breast Cancer Clinic, Ankara, Turkey*

Abstract

Objectives: This prospective study was planned to compare the predictive value of dynamic ^{18}F-fluorodeoxyglucose (FDG) positron emission tomography/computed tomography (PET/CT) in locally advanced breast cancer patients (LABC) receiving neoadjuvant chemotherapy (NAC).

Methods: Twenty seven patients with LABC [median age: 47, (26-66)] underwent a dynamic ^{18}F-FDG PET study at baseline, and after 2-3 cycles of (NAC) were included (interim). Maximum standardized uptake value (SUV_{max}) values and SUV ratios for the 2nd, 5th, 10th, and 30th minutes and dynamic curve slope (SL) values and SL ratios were measured using ^{18}F-FDG dynamic data. In addition, the values of SUV_{mean} (2minSUVmean), SULpeak (2minSULpeak), metabolic volume (2minVol), and total lesion glycolysis (2minTLG) were measured for the first 2 min. Percent changes between baseline and interim studies were calculated and compared with the pathological results as the pathological complete response (PCR) or the pathological non-complete response (non-PCR). Receiver operating characteristic curves were obtained to calculate the area under the curve to predict PCR. Optimal threshold values were calculated to discriminate between PCR and non-PCR groups.

Results: Baseline study SUV 30 (p=0.044), SUV 30/2 (p=0.041), SUV 30/5 (p=0.049), SUV 30/10 (p=0.021), SL 30/2 (p=0.029) and SL 30/5 (p=0.027) values were statistically significant different between PCR and non-PCR groups. The percentage changes of 2minVol between PCR and non-PCR groups were statistically significant. For the threshold value of -67.6% change in 2minVol, the sensitivity, specificity, positive predictive value, negative predictive value, and accuracy were 87.2%, 77.8%, 63.6%, 93.3%, and 80.7%, respectively (area under the curve: 0.826, p=0.009).

Conclusion: Semiquantitative parameters for dynamic ^{18}F-FDG PET can predict PCR. % changes in 2minVol can identify non-responding patients better than other parameters.

Keywords: Breast cancer, dynamic positron emission tomography, fluorodeoxyglucose, neoadjuvant therapy

Öz

Amaç: Bu prospektif çalışmada neoadjuvan kemoterapi (NAC) alan lokal ileri meme kanseri hastalarda (LABC) dinamik ^{18}F-florodeoksiglukoz (FDG) pozitron emisyon tomografisi/bilgisayarlı tomografinin (PET/BT), NAC yanıt öngörüsünü araştırdık.

Yöntem: LABC'li 27 hastaya [medyan yaş: 47, (26-66)] NAC öncesi ve 2-3 kür kemoterapi sonrası dinamik ^{18}F-FDG PET çalışması uyguladık. Dinamik çalışmanın 2., 5., 10 ve 30. dakikalarında maksimum standartlaştırılmış alım değeri (SUV_{maks}) değerleri, SUV oranları ile dinamik eğri eğim (SL)

Address for Correspondence: Osman Kupik MD, Muğla Training and Research Hospital, Clinic of Nuclear Medicine, Muğla, Turkey
Phone: +90 252 214 13 23 **E-mail:** osmankupik@gmail.com ORCID ID: orcid.org/0000-0001-9473-7940
Received: 29.08.2022 **Accepted:** 18.12.2022

değerleri ve SL oranları, ^{18}F-FDG dinamik verileri kullanılarak ölçüldü. Ayrıca ilk 2 dakika için SUVmean (2minSUVmean), SULpeak (2minSULpeak), metabolik volume (2minVol), and total lezyon glikoliz (2minTLG) değerlerini hesapladık. Parametrelerin tedavi öncesi ve interim çalışma arasındaki yüzde değişimlerini hesapladık ve patolojik sonuçlar [patolojik tam yanıt (PCR) olan ve olmayan (non-PCR)] ile karşılaştırdık. Parametrelerin patolojik yanıtı (PCR ve non-PCR) ayırt edebilmesi için ROC eğrisi kullanarak en uygun eşik değerleri hesapladık.

Bulgular: Tedavi öncesi SUV 30 (p=0,044), SUV 30/2 (p=0,041), SUV 30/5 (p=0,049), SUV 30/10 (p=0,021), SL 30/2 (p=0,029) ve SL 30/5 (p=0,027) değerleri PCR ve non-PCR hasta grupları arasında istatistiksel anlamlı farklı idi. Yüzde (%) değişim 2minVol, PCR ve non-PCR hasta grupları arasında istatistiksel olarak anlamlı farklılık vardı. 2minVol'deki -%67,6 değişim eşik değeri için duyarlılık %87,2, özgüllük %77,8, pozitif öngörü değeri %63,6, negatif öngörü değeri %93,3 ve doğruluk %80,7 idi (eğrinin altındaki alan: 0,826, p=0,009).

Sonuç: Dinamik ^{18}F-FDG PET parametreleri patolojik yanıtı öngörebilir. 2minVol'deki % değişiklikler, non-PCR hastaları diğer parametrelerden daha iyi belirleyebilir.

Anahtar kelimeler: Meme kanseri, dinamik pozitron emisyon tomografi, fluorodeoksiglukoz, neoadjuvan tedavi

Introduction

Neoadjuvant chemotherapy (NAC) is administered as a standard treatment for locally advanced breast cancer. Some of the main goals of NAC are to increase the rate of breast-conserving surgery and to predict the prognosis by monitoring the response of the tumor to treatment (1,2). The pathological complete response (PCR) in breast cancer patients receiving NAC is an important indicator of disease-free and overall survival (3,4).

Response to NAC is essential to be predicted at an early stage. Because in patients who do not respond to NAC it may be possible to change ineffective chemotherapy to minimize its toxic effects and prevent unnecessary costs. Successful results have been obtained in predicting the response to NAC with ^{18}F-fluorodeoxyglucose (FDG) positron emission tomography/computed tomography (PET/CT), which evaluates the metabolic activity of the tumor (5).

Obtaining dynamic data with ^{18}F-FDG enables a more detailed quantitative analysis of ^{18}F-FDG kinetics. Classically, a dynamic study requires recording 60 minute serial images and quantitatively evaluating the obtained data using a 2-compartment analysis. Various studies have shown that dynamic analysis is superior to semiquantitative analysis, with only standardized uptake values (SUV) in the diagnostic evaluation of the tumor and the follow-up of the response to treatment (6). Dynamic studies with ^{18}F-FDG have become uptodate again in recent years. Publications are increasingly applying clinical studies in a shorter time and with different analysis methods (7,8,9,10).

This prospective study investigated the success of baseline and interim dynamic PET parameters and percentage changes between them in predicting NAC response in patients with locally advanced breast cancer (LABC).

Materials and Methods

Study Cohort

We included 41 patients [median age: 47 years old, (26-66)] diagnosed with LABC and planned to receive NAC. Ethics Committee approval was obtained from Hacettepe University Faculty of Medicine (approval no: GO 13/45-29). We included patients with stage IIB, IIIA, IIIB, or IIIC according to the staging criteria of the American Joint Committee on Cancer 7th edition (11) without distant metastases and with ^{18}F-FDG uptake by a primary tumor in baseline imaging. Written informed consent forms were obtained from the patients who agreed to participate in the study. We did not include uncooperative patients or patients with uncontrolled diabetes mellitus. In addition, we excluded patients with dose infiltration and suboptimal image quality. Breast cancer diagnosis in all patients was confirmed histopathologically from biopsy materials. Estrogen, progesterone, and HER2 receptor determination were evaluated immunohistochemically. We grouped the patients as those with PCR or pathological non-complete response (non-PCR) according to the results of the histopathological evaluation. Patients were scanned with ^{18}F-FDG PET/CT before treatment (baseline), after 2-3 cycles of NAC (interim), and after the end of treatment, before surgery.

Imaging Protocol: Patients laid comfortably in the prone position with arms raised and breasts droop. A unique breast coil produced for this study was used. Attention was paid to fast for a minimum of 6 h before imaging and a maximum blood glucose 170 mg/dL during the injection. Dynamic images were obtained in a single bed position, including the primary tumor and the axilla, starting immediately after ^{18}F-FDG injection from the arm on the opposite side of the breast tumor or lower extremity. Dynamic phase images were recorded for 32 min, including ten frames of 30 min, five frames of 1 min, five frames of 2 min each, and four frames of 3 min (12). Iterative image processing was applied to the images (2 iterations, 21 subsets). CT images were obtained using a 4-slice device (140 kV, 80 mA), and attenuation correction was made with CT slices.

Data Analysis: Two nuclear medicine physicians with more than 20 years of expertize and a research assistant

performed the images at the AW-46 workstation. We evaluated the obtained dynamic images using the "DynamicVue" program on the Advantage workstation (GE Healthcare, USA). We obtained time-activity curves by plotting areas of interest on the lesion, symmetrical breast tissue, and aorta in the plane where the primary lesion is most prominent (Figure 1).

We first evaluated the curves visually. For semiquantitative evaluation, we measured SUV_{max} values (SUVmax2, SUVmax5, SUVmax10, SUVmax30) for the 2nd, 5th, 10th, and 30th minutes (Figure 2).

The slope (SL) values of the time-activity curves were calculated separately for the 0-2, 0-5, 0-10, and 0-30 minutes time periods of the obtained curves (SL2, SL5, SL10, SL30).

In addition, SUV_{mean} (2minSUV), SULpeak (2minSULpeak), volume (2minVol), and total glycolytic index (2minTLG) values were calculated by combining images taken between 0 and 2 min.

The percentage change of all measured numerical parameters after 2-3 cycles was c alculated according to the following formula [% change = (value after chemotherapy - baseline value) / baseline value x 100].

Statistical Analysis

The conformity of the variables to the normal distribution was examined with the Kolmogorov-Smirnov test. Continuous variables were expressed as median (minimum-maximum) and mean with standard deviation. Chi-square, Fisher's Exact, t-test, or Mann-Whitney U tests were used, depending on the analysis of NAC response with univariate analyses. The diagnostic decision-making properties of the calculated parameters in predicting the surgical response were analyzed by Receiver operating characteristic curve (ROC) analysis. The sensitivity, specificity, positive and negative predictive values, and accuracy were calculated in the presence of significant threshold values. P values <0.05 was considered statistically significant. Statistical analysis were performed using SPSS 18.

Results

Study Cohort: We performed baseline imaging in 29 patients and interim imaging in 41 patients and analyzed 27 patients [median age: 47, (26-66)] with baseline and interim imaging. The histopathological diagnosis of 22 patients was invasive ductal carcinoma, and five was mixed type (ductal + lobular) invasive carcinomas. While the primary tumor was unifocal in 23 patients, it was multicentric/multifocal in 4. Tumor size ranged from 16 to 96 mm (median: 44 mm). One patient had T1, 12 patients had T2, 12 patients had T3 and two had T4 tumors. The tumors of 13 patients were grade 2, while 14 was grade 3. Eighteen patients were in the hormone receptor-positive group, 4 in the TN group, and 5 in the HER2+ group. Ten patients were postmenopausal and 17 were premenopausal. There was no difference in the distribution between the groups according to receptor and menopausal status. The clinical information of the patients is given in Table 1.

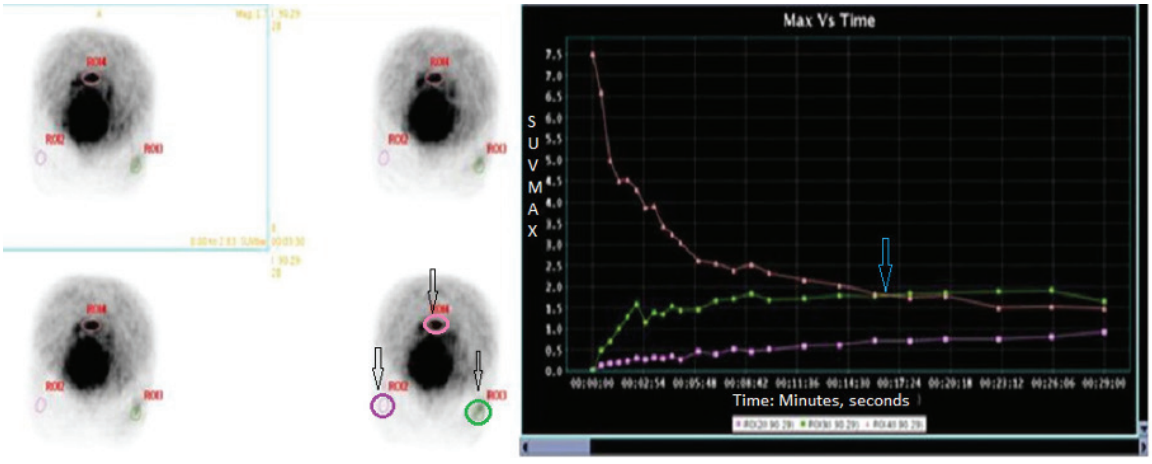

Figure 1. Time-activity curves. Right breast IDC, grade 2 tumor, 63 years-old patient. Patient was on the prone position. A green ROI was drawn to the right breast tumor, a purple ROI to the contralateral breast tissue, and a pink ROI to the aorta. Arrows indicate all three ROIs. The SUV_{max}-time graph is shown on the right. The SUV_{max}-time curve of each ROI is shown in the same color. While the contralateral breast tissue draws a low-slope SUV-time curve at the end of 29 minutes (purple curve), the tumor shows a significant SUV-time increase compared to normal tissue (green curve). While the SUV value in the aorta is initially high, it decreases rapidly over time (pink curve). At approximately 16 minutes, the aorta and tumor curves intersect (blue arrow)

IDC: Invasive ductal carcinoma, mixt, invasive ductal and lobular carcinoma, ROI: Region of interest, SUV_{max}: Maximum standardized uptake value

Surgical Response Assessment: One patient did not want to be operated on after NAC, and the remaining 26 patients underwent modified radical mastectomy. PCR was detected in 8 patients. In the remaining 18 patients, residual tumors ranging from 10 to 70 mm (median: 30 mm) were observed.

Neoadjuvant Chemotherapy Regimen: The chemotherapy regimen included four cycles of adriamycin and cyclophosphamide every 21 days, followed by weekly paclitaxel for 12 weeks. Patients with HER2+ breast cancer also received concomitant weekly trastuzumab with paclitaxel.

Baseline Study: SUV2, SUV5, SUV10, and SUV30 tumor and contralateral breast tissue values increased significantly (p=0.0001) (Figure 3). Tumor/contralateral breast SUV ratios did not change significantly over time. Figure 4 shows tumor and contralateral breast tissue dynamic SUV values and tumor/contralateral breast tissue SUV ratios

Response to Neoadjuvant Chemotherapy

SUV Values (2, 5, 10, and 30 minutes): We calculated the percentage changes in SUV values in 26 patients with complete baseline and interim data. Eight of 26 patients had a PCR, and 18 had a residual tumor. We did not find a statistically significant difference in baseline and interim study SUV values between the PCR and non-PCR groups. In addition, there was no statistically significant difference in the percentage change of SUV values. Only the baseline study SUV30 differed significantly between the groups (p=0.44). The baseline SUV30 value was higher in the PCR group (Table 2).

SUV Ratios: Baseline and interim ratio values were statistically different (p<0.001). There was a statistically significant difference in baseline SUV 30/2, 30/5, and 30/10 values between groups with and without PCR (p=0.041, 0.049, 0.021, respectively). SUV rates were higher in the PCR group (Table 3).

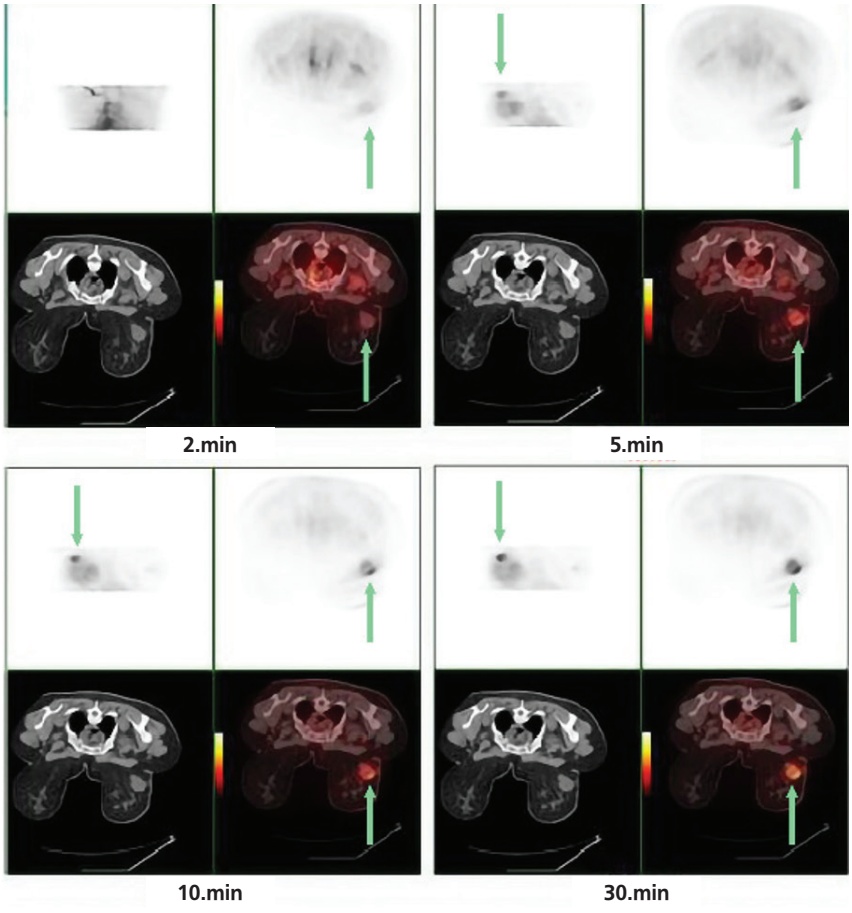

Figure 2. Right breast IDC grade 3 tumor, 56 years-old patient. Images at the 2^{nd,} 5th, 1^{0th} and 30th minutes were obtained using data acquired in the dynamic phase. Arrows indicate the same tumor
IDC: Invasive ductal carcinoma, mixt, invasive ductal and lobular carcinoma

Table 1. Patients characteristics

Patient no	Age	Histology	Tumor grade	ER	PR	HER-2	Menopause status	T	N	Tumor focality
1	43	IDC	2	+	+	-	Pre	2	1	Multifocal
2	49	IDC	2	+	+	-	Post	2	1	Unifocal
3	66	IDC	2	+	+	-	Post	2	1	Unifocal
4	32	IDC	2	+	-	-	Pre	3	1	Unifocal
5	48	Mixt	3	+	+	-	Pre	2	0	Unifocal
6	65	IDC	3	+	+	-	Post	2	1	Unifocal
7	66	IDC	2	+	+	-	Post	2	0	Unifocal
8	47	Mixt	2	+	+	-	Pre	3	3	Unifocal
9	56	IDC	3	-	-	-	Post	3	2	Unifocal
10	56	Mixt	2	+	+	-	Post	3	3	Multifocal
11	36	IDC	2	+	-	-	Pre	2	1	Unifocal
12	32	Mixt	3	-	-	-	Pre	3	3	Unifocal
13	48	IDC	3	-	-	-	Post	1b	2	Multifocal
14	32	IDC	2	+	-	+	Pre	3	1	Unifocal
15	63	IDC	3	+	+	-	Post	2	1	Unifocal
16	44	Mixt	2	-	-	+	Pre	3	3	Unifocal
17	33	IDC	3	+	+	-	Pre	3	1	Unifocal
18	40	IDC	2	+	+	-	Pre	2	1	Unifocal
19	46	IDC	3	+	+	-	Pre	3	1	Unifocal
20	28	IDC	2	-	-	+	Pre	3	1	Multifocal
21	41	IDC	2	+	+	-	Pre	3	3	Unifocal
22	56	IDC	3	-	-	+	Post	2	0	Unifocal
23	52	IDC	3	-	-	+	Pre	4	1	Unifocal
24	39	IDC	3	+	+	-	Pre	3	3	Unifocal
25	26	IDC	3	-	-	-	Pre	2	3	Unifocal
26	37	IDC	3	-	-	+	Pre	4	2	Unifocal
27	54	IDC	3	-	-	+	Post	2	2	Unifocal

ER: Estrogen receptor, PR: Progesterone receptor, HER-2: Human epidermal growth factor receptor 2, IDC: Invasive ductal carcinoma, mixt, invasive ductal and lobular carcinoma

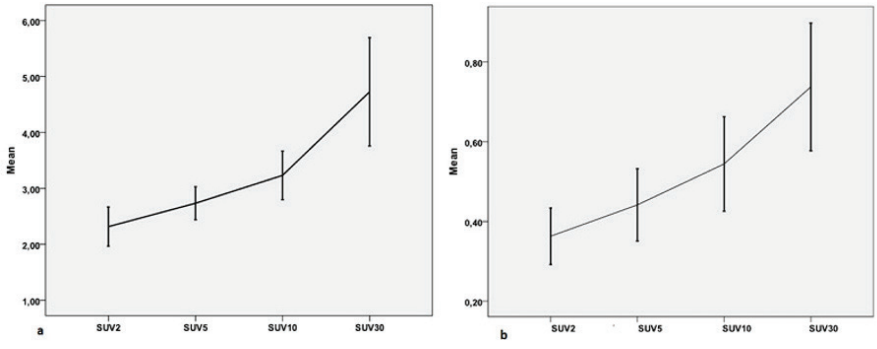

Figure 3. Increase in tumor (a) and contralateral breast tissue (b) SUV values over time in the baseline study
SUV: Maximum standardized uptake value

Dynamic Curve Slope Values: From the second minute to the 30th minute, tumor SL values showed a statistically significant decrease (p<0.001). There was no statistically significant difference in tumor SL values between groups with and without PCR (Table 4).

Slope Ratios: Baseline and interim SL ratios were statistically different (p<0.001). Baseline study SL 30/2 and SL 30/5 values significantly differed between the PCR and non-PCR groups (p=0.029 and 0.027, respectively). The values were higher in the PCR group (Table 5).

0-2 Minutes Values: 2minSUVmean, 2minSUVpeak, 2minTLG, and 2minVol values obtained from the 2nd minute of dynamic data were statistically different in baseline and interim study (p<0.001). Only percentage change 2minVol was statistically different between the PCR and non-PCR groups (p=0.009). The percentage change 2minVol values were higher in the non-PCR group (-84.8% vs. -52.55%) (Table 6).

We performed ROC analysis prediction of 2 minVol for PCR (area under the curve: 0.826, p=0.009). For the threshold value of -67.6% change, the sensitivity, specificity, positive predictive value, negative predictive value, and accuracy were 87.2%, 77.8%, 63.6%, 93.3%, and 80.7%, respectively.

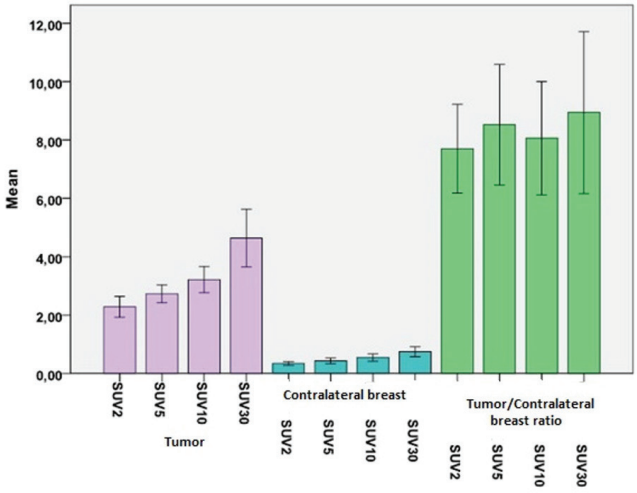

Figure 4. Tumor and contralateral breast tissue SUV values and tumor/contralateral SUV ratios
SUV: Maximum standardized uptake value

Discussion

This study investigated dynamic ^{18}F-FDG parameters predicting NAC response in patients with LABC. In dynamic imaging, ^{18}F-FDG uptake of tumor and normal breast tissue increased with time. While the SUV value in the tumor tissue was 2 on average in the 2nd minute, it increased to 5 in a short time. It was observed that the SUV value in normal breast tissue increased from 0.4 to around 0.8 within 30 min. Thus, in 30 min, tumor tissue shows ^{18}-FDG uptake at a rate of 6-10 times compared to normal tissue. Only a few groups are working on the dynamic study of breast cancer and prediction of NAC response, and generally with small patient groups (8,13,14,15).

A study comparing dynamic ^{18}F-FDG PET/CT with standard whole-body ^{18}F-FDG PET/CT in predicting response to NAC showed that K1 and Ki values were more accurate than SUV values and were associated with overall survival and disease-free survival (8). In multivariate analysis, K1 was the only independent predictor of survival. Thus, the dynamic study was more advantageous than the standard

Table 2. Baseline and interim study SUV values, % changes, and their relation with pathological complete response

Parameter	Imaging	All patients	PCR	non-PCR	p
SUV2min	Baseline	2.37 (0.50, 4.53)	2.195 (0.96, 4.53)	2.47 (1.04, 3.90)	NS
	Interim	0.80 (0.1, 4.27)	0.77 (0.1, 3.32)	0.98 (0.14, 3.88)	NS
	Change %	-46.19 (-93.01, 53.22)	-58.22 (-86.37, -26.74)	-45.67 (-93.01, 53.22)	NS
SUV5min	Baseline	2.85 (1.03, 3.92)	3.085 (1.48, 3.89)	2.57 (1.48, 3.92)	NS
	Interim	1.31 (0.22, 4.04)	1.11 (0.23, 3.23)	1.41 (0.22, 4.04)	NS
	Change %	-51.95 (-84.09, 38.74)	-62.14 (-84.09, -11.03)	-41.25 (-82.88, 38.74)	NS
SUV10min	Baseline	3.28 (1.27, 6.54)	3.54 (1.82, 6.54)	-41.25 (-82.88, 38.74)	NS
	Interim	1.61 (0.39, 5.15)	1.41 (0.47, 3.19)	2.82 (1.67, 5.0)	NS
	Change %	-47.02 (-88.48, 38.59)	-50.88 (-88.48, 3.84)	1.64 (0.39, 5.15)	NS
SUV30min	Baseline	4.19 (1.39, 12.20)	6.03 (2.92, 12.2)	3.78 (2.05, 8.45)	0.044
	Interim	1.97 (0.86, 6.37)	1.63 (0.86, 5.35)	2.01 (0.86, 6.37)	NS
	Change %	-43.28 (-88.57, 10.69)	-59.81 (-88.57, -22.65)	-40.28 (-69.04, 10.69)	NS

NS: Statistically non-significant, PCR: Pathological complete response, SUV: Standardized uptake value

Table 3. Baseline and interim study SUV ratio values and relationship with pathological complete response					
Parameter	**Imaging**	**All patients**	**PCR**	**non-PCR**	**p**
SUV30/2min	Baseline	1.98 (0.79, 6.57)	2.93 (1.15, 6.57)	1.94 (0.79, 5.09)	**0.041**
	Interim	2.21 (0.90, 8.45)	3 (0.90, 8.45)	2.120 (0.93, 6.12)	NS
SUV30/5min	Baseline	1.41 (0.81, 3.19)	2.05 (1.14, 3.19)	1.35 (0.99, 2.74)	**0.049**
	Interim	1.570 (0.92, 4.0)	1.790 (0.92, 3.68)	1.515 (0.97, 4)	NS
SUV30/10min	Baseline	1.34 (0.84, 2.0)	1.65 (1.11, 20)	1.27 (0.84, 1.90)	**0.021**
	Interim	1.19 (0.88, 2.36)	1.19 (0.88, 2.36)	1.205 (0.98, 2.22)	NS
NS: Statistically non-significant, PCR: Pathological complete response, SUV: Standardized uptake value					

Table 4. Baseline and interim study slope values. Relationship with the pathological complete response					
Parameter	**Imaging**	**All patients**	**PCR**	**non-PCR**	**p**
Slope 2min	Baseline	0.0173 (0.0042, 0.214)	0.0158 (0.0074, 0.034)	0.0186 (0.0075, 0.214)	NS
	Interim	0.0068 (0.0008, 0.0329)	0.0058 (0.0008, 0.0158)	0.0078 (0.0010, 0.0270)	NS
Slope 5min	Baseline	0.0069 (0.0018, 0.0125)	0.0068 (0.0039, 0.0119)	0.0072 (0.0018, 0.0125)	NS
	Interim	0.0040 (0.0006, 0.008)	0.0034 (0.0008, 0.0059)	0.0042 (0.0006, 0.008)	NS
Slope 10min	Baseline	0.0034 (0, 0.0096)	0.0033 (0.002, 0.0096)	0.0034 (0, 0.0065)	NS
	Interim	0.0019 (0.0004, 0.005)	0.0014 (0.0007, 0.0037)	0.002 (0.0004, 0.005)	NS
Slope 30min	Baseline	0.0013 (-0.0001, 0.0065)	0.0025 (0.0006, 0.0065)	0.0012 (-0.0001, 0.0039)	NS
	Interim	0.0007 (-0.0003, 0.006)	0.0007 (0, 0.0024)	0.0012 (-0.0001, 0.0039)	NS
NS: Statistically non-significant, PCR: Pathological complete response					

Table 5. Baseline and interim study slope ratio values. Relationship with the pathological complete response					
Parameter	**Imaging**	**All patients**	**PCR**	**non-PCR**	**p**
Slope 30/2min	Baseline	0.1 (-0.01, 0.42)	0.19 (0.03, 0.42)	0.09 (0, 0.30)	0.029
	Interim	0.12 (-0.01, 0.98)	0.19 (0.3, 0.75)	0.115 (-0.1, 0.98)	NS
Slope 30/5min	Baseline	0.21 (0.04, 0.55)	0.47 (0.11, 0.55)	0.19 (0.04, 0.44)	0.027
	Interim	0.25 (-0.05, 2.14)	0.29 (0, 0.75)	0.235 (-0.5, 2.1)	NS
Slope 30/10min	Baseline	0.48 (0.15, 0.83)	0.675 (0.27, 0.78)	0.42 (0.15, 0.83)	NS
	Interim	0.42 (-0.25, 3.0)	0.43 (0.02, 0.86)	0.42 (-0.25, -3)	NS
NS: Statistically non-significant, PCR: Pathological complete response					

whole-body ^{18}F-FDG PET/CT study in predicting the surgical response and prognosis. In their comparative study with 15 H_2O and ^{18}F-FDG PET/CT, the same study group showed that blood flow measured directly with 15 H_2O was correlated with K1 values measured with ^{18}F-FDG, and that K1 values were a parameter that indirectly showed blood flow (14). FDGK1 reflects glucose transport from blood to tissue and FDGKi is a flow constantly. It is assumed that ^{18}F-FDG is transported from blood to tissue at a linear transfer rate of K1 relative to blood flow. K1, a measure of capillary permeability and perfusion, has been shown to have a prognostic value in cancer therapy. A dynamic PET study in patients with soft tissue sarcoma also found a strong relationship between SUV obtained between 1.5 and 2.5 min and K1 values (r=0.79, p<0.05) (16). In a study on lung cancer, it was shown that there is a strong correlation (r=0.83, p=0001) between K1 values obtained with dynamic ^{18}F-FDG PET and early phase imaging (0-2 minutes) (17).

In our study, the perfusion parameters (2minSUV, 2minSULpeak, 2minTLG, and 2minVol) were obtained from the first 2 min images, which were created assuming that the perfusion of the tumor showed a significant decrease in response to NAC. In a study comparing contrast-enhanced dynamic MRI with dynamic ^{18}F-FDG PET/CT, the change in K1 and Ki values, the enhancement peak showing vascularity in MRI, and the change in tumor volume were compared. They found a higher rate of change in

Table 6. Pathological complete response relationship of parameters obtained from images between 0-2 minutes, and their percentage changes

Parameter	Imaging	All patients	PCR	non-PCR	p
2minSUV	Baseline	0.86 (0.16, 1.80)	1.08 (0.44, 1.8)	0.94 (0.29, 1.68)	NS
	Interim	0.32 (0, 2.08)	0.33 (0, 2.08)	0.31 (0, 1.66)	NS
2minVol	Baseline	21.27 (3.52, 151)	24.88 (4.5, 100)	17.45 (4.4, 151.0)	NS
	Interim	3.33 (0, 73.05)	1.96 (0, 21.91)	3.42 (0, 34.72)	NS
	Change %	-66.3 (-100, -22.3)	-84.8 (-100,-63.8)	-52.55 (-100, -22.3)	**0.009**
2minTLG	Baseline	17.75 0.56,226.5)	22.55 (2.88, 180)	16.35 (1.54, 226.5)	NS
	Interim	1.32 (0, 8.3)	0.55 (0, 45.6)	1.63 (0, 42.8)	NS
	Change %	-82.1 (-100, 6.5)	-95.2 (-100,-74.7)	-78.45 (-100, 6.5)	NS
2minSULpeak	Baseline	0.74 (0.1, 1.89)	0.93 (0.50, 1.89)	0.66 (0.32, 1.83)	NS
	Interim	0.24 (0, 1.86)	0.24 (0, 0.98)	0.25 (0, 1.86)	NS
	Change %	-67.9 (-100, 45.3)	-74.75 (-100, -18.3)	-64.45 (-100, 45.3)	NS

NS: Statistically non-significant, PCR: Pathological complete response, SUV: Standardized uptake value, TLG: Total lesion glycolysis

patients who fully responded to treatment (15). A two-compartment analysis of ^{18}F-FDG yields five constants: Four transport rates (k1, k2, k3, k4) describe the exchange of tracer between blood and tissue. In the case of ^{18}F-FDG, k1 reflects the influx, k2 the efflux, k3 the phosphorylation rate, and k4 the dephosphorylation rate of the glucose analog. Ki= (k1xk3/k2+k3). Through these, the metabolic rate can be quantitatively measured. However, since this process requires time and a unique computer program, we calculated the SL values of time-activity curves, which are practical for routine studies. A group working on dynamic ^{18}F-FDG studies used the SL and intercepted values obtained by linear regression analysis applied to time-activity curves as parametric images (18).

It is stated that the SL values reflect the trapping function of ^{18}F-FDG. Based on this information, we calculated the SL values in different periods of the 30-min dynamic study. While the SL values were high in the early periods, they decreased in tumor and normal breast tissue over time. At the same time, the SL values did not differ between the groups in predicting the NAC response. The values of baseline SL ratios SL30/2 and SL30/5 were higher in the PCR group.

Study Limitations

K1 and Ki values could be calculated by evaluating the kinetic analysis of dynamic studies through a special program. However, the program was not available on our workstation. A separate statistical evaluation according to receptor subgroups could not be made due to the small number of patients.

Conclusion

In conclusion, dynamic imaging is a component that can be used in specific patient groups and can be easily added to standard imaging. Semiquantitative parameters for dynamic ^{18}F-FDG can predict the response to NAC. Percentage changes in 2 minVol can identify non-responding patients.

Ethics

Ethics Committee Approval: Ethics Committee approval was obtained from Hacettepe University Faculty of Medicine (approval no: GO 13/45-29).

Informed Consent: Written informed consent forms were obtained from the patients who agreed to participate in the study.

Peer-review: Externally and internally peer-reviewed.

Authorship Contributions

Concept: O.K., M.T., P.Ö.K., M.G.A., K.A., F.B.D., B.E., Design: O.K., M.T., M.G.A., K.A., F.B.D., B.E., Data Collection or Processing: O.K., M.T., P.Ö.K., M.G.A., K.A., F.B.D., B.E., Analysis or Interpretation: O.K., B.E., Literature Search: O.K., B.E., Writing: O.K., B.E.

Conflict of Interest: No conflict of interest was declared by the authors.

Financial Disclosure: The authors declared that this study has received no financial support.

References

1. Wolff AC, Davidson NE. Primary systemic therapy in operable breast cancer. J Clin Oncol 2000;18:1558-1569.
2. Rastogi P, Anderson SJ, Bear HD, Geyer CE, Kahlenberg MS, Robidoux A, Margolese RG, Hoehn JL, Vogel VG, Dakhil SR, Tamkus D, King KM, Pajon ER, Wright MJ, Robert J, Paik S, Mamounas EP, Wolmark N. Preoperative

chemotherapy: updates of National Surgical Adjuvant Breast and Bowel Project Protocols B-18 and B-27. J Clin Oncol 2008;26:778-785.

3. Kuerer HM, Newman LA, Smith TL, Ames FC, Hunt KK, Dhingra K, Theriault RL, Singh G, Binkley SM, Sneige N, Buchholz TA, Ross MI, McNeese MD, Buzdar AU, Hortobagyi GN, Singletary SE. Clinical course of breast cancer patients with complete pathologic primary tumor and axillary lymph node response to doxorubicin-based neoadjuvant chemotherapy. J Clin Oncol 1999;17:460-469.
4. Buzdar AU, Ibrahim NK, Francis D, Booser DJ, Thomas ES, Theriault RL, Pusztai L, Green MC, Arun BK, Giordano SH, Cristofanilli M, Frye DK, Smith TL, Hunt KK, Singletary SE, Sahin AA, Ewer MS, Buchholz TA, Berry D, Hortobagyi GN. Significantly higher pathologic complete remission rate after neoadjuvant therapy with trastuzumab, paclitaxel, and epirubicin chemotherapy: results of a randomized trial in human epidermal growth factor receptor 2-positive operable breast cancer. J Clin Oncol 2005;23:3676-3685.
5. Tian F, Shen G, Deng Y, Diao W, Jia Z. The accuracy of 18F-FDG PET/CT in predicting the pathological response to neoadjuvant chemotherapy in patients with breast cancer: a meta-analysis and systematic review. Eur Radiol 2017;27:4786-4796.
6. Dimitrakopoulou-Strauss A, Strauss LG, Egerer G, Vasamiliette J, Mechtersheimer G, Schmitt T, Lehner B, Haberkorn U, Stroebel P, Kasper B. Impact of dynamic 18F-FDG PET on the early prediction of therapy outcome in patients with high-risk soft-tissue sarcomas after neoadjuvant chemotherapy: a feasibility study. J Nucl Med 2010;51:551-558.
7. Strauss LG, Pan L, Cheng C, Haberkorn U, Dimitrakopoulou-Strauss A. Shortened acquisition protocols for the quantitative assessment of the 2-tissue-compartment model using dynamic PET/CT 18F-FDG studies. J Nucl Med 2011;52:379-385.
8. unnwald LK, Doot RK, Specht JM, Gralow JR, Ellis GK, Livingston RB, Linden HM, Gadi VK, Kurland BF, Schubert EK, Muzi M, Mankoff DA. PET tumor metabolism in locally advanced breast cancer patients undergoing neoadjuvant chemotherapy: value of static versus kinetic measures of fluorodeoxyglucose uptake. Clin Cancer Res 2011;17:2400-2409.
9. Payan N, Presles B, Brunotte F, Coutant C, Desmoulins I, Vrigneaud JM, Cochet A. Biological correlates of tumor perfusion and its heterogeneity in newly diagnosed breast cancer using dynamic first-pass 18F-FDG PET/CT. Eur J Nucl Med Mol Imaging 2020;47:1103-1115.
10. Kajáry K, Lengyel Z, Tőkés AM, Kulka J, Dank M, Tőkés T. Dynamic FDG-PET/CT in the initial staging of primary breast cancer: clinicopathological correlations. Pathol Oncol Res 2020;26:997-1006.
11. Edge SB, Compton CC. The American Joint Committee on Cancer: the 7th edition of the AJCC cancer staging manual and the future of TNM. Ann Surg Oncol 2010;17:1471-1474.
12. Strauss LG, Koczan D, Klippel S, Pan L, Willis S, Sachpekidis C, Dimitrakopoulou-Strauss A. Dynamic PET with (18)F-Deoxyglucose (FDG) and quantitative assessment with a two-tissue compartment model reflect the activity of glucose transporters and hexokinases in patients with colorectal tumors. Am J Nucl Med Mol Imaging 2013;3:417-424.
13. Specht JM, Kurland BF, Montgomery SK, Dunnwald LK, Doot RK, Gralow JR, Ellis GK, Linden HM, Livingston RB, Allison KH, Schubert EK, Mankoff DA. Tumor metabolism and blood flow as assessed by positron emission tomography varies by tumor subtype in locally advanced breast cancer. Clin Cancer Res 2010;16:2803-2810.
14. Dunnwald LK, Gralow JR, Ellis GK, Livingston RB, Linden HM, Specht JM, Doot RK, Lawton TJ, Barlow WE, Kurland BF, Schubert EK, Mankoff DA. Tumor metabolism and blood flow changes by positron emission tomography: relation to survival in patients treated with neoadjuvant chemotherapy for locally advanced breast cancer. J Clin Oncol 2008;26:4449-4457.
15. Partridge SC, Vanantwerp RK, Doot RK, Chai X, Kurland BF, Eby PR, Specht JM, Dunnwald LK, Schubert EK, Lehman CD, Mankoff DA. Association between serial dynamic contrast-enhanced MRI and dynamic 18F-FDG PET measures in patients undergoing neoadjuvant chemotherapy for locally advanced breast cancer. J Magn Reson Imaging 2010;32:1124-1131.
16. Rusten E, Rødal J, Revheim ME, Skretting A, Bruland OS, Malinen E. Quantitative dynamic ^{18}FDG-PET and tracer kinetic analysis of soft tissue sarcomas. Acta Oncol 2013;52:1160-1167.
17. Tuncel M, Kupik O, Kiratli P, Erbas B. Practical measures of dynamic 18 FDG time-activiy curves. Eur J Nucl Med Mol Imaging. 2015(Suppl 1):375.
18. Dimitrakopoulou-Strauss A, Pan L, Strauss LG. Quantitative approaches of dynamic FDG-PET and PET/CT studies (dPET/CT) for the evaluation of oncological patients. Cancer Imaging 2012;12:283-289.